EUROPEAN ORGANIZATION FOR NUCLEAR RESEARCH

CERN-PPE/91-228
13 December 1991

Transverse Momentum Distributions for Exclusive ρ^0 Muoproduction

THE NEW MUON COLLABORATION (NMC)

Bielefeld University[1+], *CERN*[2], *Freiburg University*[3+], *Max-Planck Institut für Kerphysik, Heidelberg*[4+], *Heidelberg University*[5+], *Mainz University*[6+], *Mons University*[7], *Neuchâtel University*[8], *NIKHEF-K*[9++], *Oxford University*[10], *University of California, Santa Cruz*[11], *Paul Scherrer Institute*[12], *Torino University and INFN Torino*[13], *Uppsala University*[14], *Istitute for Nuclear Studies, Warsaw*[15*], *Warsaw University*[16**], *Wuppertal University*[17+]

P. Amaudruz[12a)], M. Arneodo[13], A. Arvidson[14], B. Badełek[16], G. Baum[1], J. Beaufays[9b)], I.G. Bird[4c)], M. Botje[12], C. Broggini[8d)], W. Brückner[4], A. Brüll[3], W.J. Burger[12e)], J. Ciborowski[16], R. van Dantzig[9], H. Döbbeling[4f)], J. Domingo[12g)], J. Drinkard[11], H. Engelien[3], M.I. Ferrero[13], L. Fluri[8], P. Grafstrom[14h)], D. von Harrach[4i)], M. van der Heijden[9], C. Heusch[11], Q. Ingram[12], K. Janson[14], M. de Jong[9], E.M. Kabuß[4i)], R. Kaiser[3], T.J. Ketel[9], F. Klein[6], B. Korzen[17], U. Krüner[17], S. Kullander[14], U. Landgraf[3], F. Lettenström[11], T. Lindqvist[14], G.K. Mallot[6], C. Mariotti[13], G. van Middelkoop[2,9], Y. Mizuno[4j)], J. Nassalski[15], D. Nowotny[4k)], N. Pavel[17l)], C. Peroni[13], H. Peschel[17m)], B. Povh[4,5], R. Rieger[6], K. Rith[4], K. Röhrich[6n)], E. Rondio[16], L. Ropelewski[16], A. Sandacz[15], C. Scholz[4], R. Schumacher[12o)], U. Sennhauser[12p)], F. Sever[1q)], T.-A. Shibata[5], M. Siebler[1], A. Simon[4], A. Staiano[13], G. Taylor[10r)], M. Treichel[4s)], J.L. Vuilleumier[8], T. Walcher[6], R. Windmolders[7], F. Zetsche[4]

(submitted to Zeitschrift für Physik)

Abstract

We have studied transverse momentum distributions for exclusive ρ^0 muoproduction on protons and heavier nuclei at $2 < Q^2 < 25$ GeV^2. The Q^2 dependence of the slopes of the p_t^2 and t' distributions is discussed. The influence of the non-exclusive background is investigated. The p_t^2-slope for exclusive events is $4.3 \pm 0.6 \pm 0.7$ GeV^{-2} at large Q^2. The p_t^2 spectra are much softer than inclusive p_t^2 spectra of leading hadrons produced in deep inelastic scattering.

For footnotes see next page

+ Supported by Bundesministerium für Forschung und Technologie.
++ Supported in part by FOM, Vrije Universiteit Amsterdam and NWO.
* Supported by CPBP.01.06.
** Supported by CPBP.01.09.

a) Now at TRIUMF, Vancouver, BC V6T 2A3, Canada.
b) Now at Trasys, Brussels, Belgium.
c) Now at NIKHEF-K, P.O. BOX 4395, 1009 AJ Amsterdam, The Netherlands.
d) Now at INFN, Laboratori Nazionali del Gran Sasso, 67010 Assergi, Italy.
e) Now at Université de Genève, 1211 Genève 4, Switzerland.
f) Now at GSI, W-6100 Darmstadt, Germany.
g) Now at CEBAF, Newport News, VA 23606, U.S.A.
h) Now at CERN, 1211 Genève 23, Switzerland.
i) Now at University of Mainz, W-6500 Mainz, Germany.
j) Now at Osaka University, 567 Osaka, Japan.
k) Now at SAP AG, W-6909 Walldorf, Germany.
l) Now at DESY, W-2000 Hamburg 52, Germany.
m) Now at Gruner und Jahr AG & CoKG, W-2210 Itzehoe, Germany.
n) Now at IKP2-KFA, W-5170 Jülich, Germany.
o) Now at Carnegie Mellon University, Pittsburgh, PA 15213, U.S.A.
p) Now at EMPA, 8600 Dübendorf, Switzerland.
q) On leave from Jozef Stefan Institut, Ljubljana, Slovenia.
now at DPhN Saclay, 91191 Gif-sur-Yvette, France.
r) Now at University of Melbourne, Parkville, Victoria, Australia.
s) Now at Université de Neuchâtel, 2000 Neuchâtel, Switzerland.

Introduction

In this paper we present new results on the p_t^2 and t' distributions ($t' = |t - t_{min}|$) for ρ^0 mesons produced in the process $\gamma^* N \to \rho^0 N$. The data come from large Q^2 muon scattering on protons and heavier nuclei measured by the New Muon Collaboration (CERN - NA37).

In the region of small Q^2 there exist numerous experimental data on exclusive vector meson electroproduction (for a review see ref. [1]). In contrast, there are only a few experimental results on exclusive ρ^0 production at large Q^2 (> 5 GeV^2). The latter are from deep inelastic muon scattering on hydrogen [2] and ammonia [3], both measured by the European Muon Collaboration.

Exclusive vector meson electro-/muoproduction, especially at large Q^2, plays an important role in investigations of pomeron exchange and its possible interpretation in terms of multiple gluon exchange [4-7]. While a substantial part of the information on pomeron properties is obtained from soft hadronic processes (total cross sections, elastic scattering, diffraction dissociation), processes at large Q^2 are expected to yield additional information. It has been suggested that from the Q^2 dependence of the cross section for exclusive ρ^0 production information on the pomeron "size" can be deduced [4,6]. Further, if one interprets the pomeron in terms of the exchange of two non-perturbative gluons [6-8], then in this process the relative contributions of different two-gluon exchange diagrams varies with Q^2. The sum of all contributions may be represented by a pomeron form factor, whose shape is determined by a gluon confinement length [6].

The EMC data on exclusive ρ^0 muoproduction from hydrogen have been used to test such phenomenological [4] and QCD-inspired [7] models which assume dominant contributions from pomeron exchange. The agreement was generally satisfactory and it was deduced that the "size" of pomeron is about 1 GeV^{-1} [4,6,7]. However, one aspect of the EMC data is not understood. Whereas the predicted t' distributions have rather large slopes (> 5 GeV^{-2}), the measured t'-slopes decrease with increasing Q^2 to values of 1.5–2 GeV^{-2} at $Q^2 > 7$ GeV^2 [2,3], which was taken as an indication that at large Q^2 exclusive muoproduction becomes a hard scattering process [2].

The purpose of the present work is to resolve the previous apparent discrepancy between experiment and model predictions of t'-slopes. The enhanced statistical accuracy permits a more detailed investigation of kinematical distributions and background.

Experiment and Analysis

The experiment was performed at the M2 muon beam at the CERN SPS. The upgraded version of the EMC forward spectrometer [9] was used to detect incident and scattered muons as well as forward produced hadrons. The apparatus had good efficiency for the detection of charged hadrons of momenta greater than 4–5 GeV.

There are two sets of data taken with different incident muon energies and target arrangements. One data set was taken at an energy of 280 GeV with hydrogen

and deuterium targets, the other one at a muon energy of 200 GeV with deuterium, carbon and calcium targets. The data were taken during five SPS periods in 1987 simultaneously with the structure function measurements [9,10].

Complementary target arrangements were used, which were primarily designed for accurate measurements of the ratios of deep inelastic cross sections from different target materials. Each target set contained several segments of different materials (either H,D [9] or D,C,Ca [10]) simultaneously exposed to the beam, one behind the other along the beam direction. The sets were frequently exchanged (every 30 min.) with complementary ones where the longitudinal positions of the target materials were interchanged. Events from different targets were well separated.

The present data on the exclusive ρ^0 production were taken with the standard trigger which accepted muons at scattering angles larger than 10 mrad.

The data were processed on an event by event basis using an upgraded version of the EMC program chain [9] which reconstructed tracks and interaction vertices. For this analysis we selected events with only two hadron tracks of opposite charge associated with the muon vertex.

The standard variables employed in deep inelastic scattering are used. These are Q^2, ν, x, y and W^2 [11]. To describe the hadronic system we also use the following variables: the missing mass squared of the recoiling system $M_X^2 = (q + p - v)^2$; the inelasticity $I = (M_X^2 - M_p^2)/W^2$; the invariant mass of the two pion system $m_{\pi\pi} = (v^2)^{\frac{1}{2}}$; the squared transverse momentum p_t^2 relative to the direction of the virtual photon; and the four momentum transfer squared $t = (q - v)^2$. Here q and p are the four-momenta of the virtual photon and the target nucleon respectively, M_p is the proton mass and $v = (p_{h^+} + p_{h^-})$ is the four-momentum of the outgoing pair of hadrons. As in this experiment there was no hadron identification, the energy of a hadron was calculated using the pion mass. In addition, we define $t' = |t - t_{min}|$, where $|t_{min}|$ is the minimum kinematically allowed $|t|$ for given W^2, Q^2, $m_{\pi\pi}$ and M_X^2.

Electrons were rejected using the information from a calorimeter [12] with an efficiency of more than 90%. The effect of removing electrons on the measured p_t^2- and t'-slopes was found to be negligible.

A Monte Carlo simulation was used to correct the data for acceptance losses, smearing and reconstruction efficiencies. The generated sample consisted of exclusive ρ^0's produced coherently and incoherently with the relative contributions depending on the atomic mass of each target. All outgoing particles, including the scattered muons and radiative photons were tracked through the target and the apparatus. Secondary interactions of hadrons inside the target, photon conversions and multiple Coulomb scattering were taken into account.

For each generated event, the responses of the detectors were simulated in full. These events were then processed in the same way as real events. The overall acceptance for a distribution in a given variable was calculated as the ratio of the distribution obtained after the event processing to the distribution for generated events. The acceptance as a function of p_t^2 changed by about 35% over the measured

p_t^2 range. This results in a correction of about 0.3 GeV^{-2} to the measured p_t^2-slopes for hydrogen and for incoherent ρ^0 production on nuclear targets. On the other hand, the observed shape of the p_t^2 distributions for coherent ρ^0 production from nuclei is strongly affected by smearing. The contribution of coherent events was found negligible above $p_t^2 = 0.2$ GeV^2.

There was no attempt to generate a background to the exclusive processes because, as discussed in [7], different fragmentation models give substantially different results. Instead, the background was estimated from the data (see next section).

Results

The exclusive ρ^0 signal is shown in Figs. 1 and 2 for the data from the D target at 200 GeV. (The other sets of data have similar distributions.)

In Fig.1 the acceptance corrected distribution of the two-pion invariant mass is given for the events satisfying the kinematic cuts listed in Table 1 and an inelasticity cut

$$-0.1 < I < 0.08. \tag{1}$$

The full line is a result of a fit assuming a superposition of a ρ^0 p-wave Breit-Wigner distribution [13] and a non-resonant contribution. The broken line represents the fitted non-resonant contribution. Satisfactory fits were obtained which yielded the ρ^0 mass and width consistent with those in the Review of Particle Properties [14]. For the central part of the ρ^0 peak, 0.62 GeV $< m_{\pi\pi} <$ 0.92 GeV, the non-resonant contribution is about 25% .

In Fig.2 the inelasticity distribution uncorrected for acceptance is shown for the data sample satisfying the cuts listed in Table 1 and a cut on the invariant mass

$$0.62\,\text{GeV} < m_{\pi\pi} < 0.92\,\text{GeV}. \tag{2}$$

The clear enhancement at $I = 0$ is the signal of exclusive ρ^0 production. The non-exclusive events contribute mostly at large inelasticity, but due to the finite resolution they cannot be completely resolved from the exclusive ρ^0 peak. This, as well as the parametrisation of the inelasticity distributions for non-exclusive events (an example is shown as a curve in Fig. 2), will be discussed later.

The numbers of events in the exclusive ρ^0 data sample are given in Table 2. These numbers result after applying the cuts listed in Table 1 and the additional cuts (1,2) on the inelasticity and the invariant mass of two pions. The number of events in our sample is about four times as large as in previous experiments in similar kinematical regions.

The average values of the kinematical variables for the data sample are $< Q^2 >$ = 6.3 GeV^2 and $< \nu >$ = 112 GeV for the 200 GeV data, and $< Q^2 >$ = 9.4 GeV^2 and $< \nu >$ = 166 GeV for the 280 GeV data. For the individual targets the average values differ from these by not more than 1 GeV^2 for $< Q^2 >$ and 4 GeV for $< \nu >$. These differences are caused by different acceptances for different targets.

We now discuss the ρ^0 distributions in the "transverse" variables, i.e. in p_t^2 and t'. Examples of acceptance corrected p_t^2 distributions for selected targets and

Q^2 bins are shown in Fig.3. For ρ^0 production on hydrogen the data are consistent with a single-exponent dependence of the differential cross section over the whole measured p_t^2 range down to zero. For deuterium the cross sections are consistent with the same type of p_t^2 behaviour, although there is an indication of a weak signal from the coherent process at smaller Q^2 values. For the calcium target the coherent signal is clearly seen at small p_t^2, with its relative contribution diminishing with increasing Q^2. Otherwise the differential cross sections have shapes similar to that for hydrogen. The full lines are fits to the data of the form

$$\frac{dN}{dp_t^2} = a\, e^{-bp_t^2}, \tag{3}$$

where a and b are fitted parameters. For all targets except hydrogen, the data in the range 0.2 GeV^2 $< p_t^2 <$ 1.5 GeV^2 were used in the fit. The lower cut was introduced to eliminate coherent events. For the hydrogen data the lower cut was removed. The t' distributions display similar features, as for the majority of exclusive events $t' \simeq p_t^2$.

The fitted p_t^2-slopes as a function of Q^2 obtained separately for each target material are shown in Fig.4. Any differences between the fitted slopes for different targets for a given Q^2 bin and incident muon energy are not statistically significant. In the following the data for all target materials taken at the same kinematical conditions are combined. In Fig.5 the Q^2 dependence of the p_t^2-slope for the combined data is shown. The errors shown are statistical. The total systematic errors (mostly due to uncertainties in the momentum calibration and acceptance corrections) are about 0.5 GeV^{-2}. Apart from the somewhat higher values at small Q^2 there is little Q^2 dependence, and the parameter b is consistent with a constant value of about 3 GeV^{-2} at large Q^2. The t'-slopes obtained in an analogous way are also shown in Fig. 5. The t' variable was calculated in the same way as in the EMC analysis, i.e. assuming that for every event in the sample the only final state hadrons were the ρ^0 meson and the unmeasured recoil nucleon. At large Q^2 the t'-slope exhibits a tendency to be smaller than the corresponding p_t^2-slope going down to about 1.5 GeV^{-2} at large Q^2 values.

Before further discussing this difference, we compare our results to those of the previous experiments performed in the large Q^2 range. In Fig.6 the t'-slopes from the present experiment are compared to those from the EMC experiments [2,3]. Our data confirm the results of the previous experiments, and in addition extend to somewhat larger Q^2.

The difference between p_t^2-slopes and t'-slopes may seem unexpected as for the majority of exclusive ρ^0 events one has $t' \simeq p_t^2$. However, for the non-exclusive background events which contribute to the sample, t' calculated assuming t_{min} as for truly exclusive events is inappropriate. The t_{min} depends on the mass of the recoiling system, so using the nucleon mass M_p in the calculations instead of the true mass may distort the t' distributions. To check if this indeed affects the t'-slopes we calculated t' assuming on an event by event basis that the mass of the

recoiling system is equal to the measured missing mass[1]. In Fig.7 t'-slopes obtained with $t_{min1} = t_{min}(M_p)$ are compared to those obtained with $t_{min2} = t_{min}(M_X)$. For the latter case the slopes at larger Q^2 values are about 1.5 GeV^{-2} bigger than for the former one, becoming close to the p_t^2-slopes. We conclude that due to the non-exclusive background in our sample, as well as in the samples of the EMC experiments, using t' distributions with t_{min} calculated with the nucleon mass leads to a distortion of t'-slope values and an extra Q^2 dependence. For this reason we prefer to use the p_t^2 variable, which is free from the uncertainty related to the mass of the recoiling system.

In the following we consider the influence of the non-exclusive background on the measured p_t^2-slopes. To obtain the values of the slopes for the exclusive events, we assumed that the observed p_t^2 distribution results from a superposition of exclusive events and a non-exclusive background. We assumed that each class of events can be described by an exponential p_t^2 dependence. In order to determine the slope b_{ex} of the p_t^2-dependence for exclusive events, it is necessary to know both the p_t^2-slope, b_{bk}, of the the non-exclusive background and the amount of non-exclusive events in the elastic region.

The background slope b_{bk} was estimated from our data in the inelastic region. The measured p_t^2-slope as a function of inelasticity for a sub-set of the data is shown in Fig.8. The presented sample consists of the combined data at both energies and for the Q^2 range 6 – 25 GeV^2. As illustrated in Fig.8, within the inelasticity range defined by cut (1) the measured slope b is not constant, but decreases towards the inelastic region as the proportion of non-exclusive events increases. In the inelastic region the p_t^2-slopes are significantly different to those in the elastic region, so that the background needs to be correctly subtracted. The slope of this background, b_{bk}, was assumed to be 1.56 ± 0.15 GeV^{-2}, which is the slope measured in the range $0.08 < I < 0.2$ (average of the four rightmost points in Fig. 8).

To estimate the amount of non-exclusive background in the elastic region the inelasticity distributions were fitted in the near inelastic region ($0.08 < I < 0.20$) with a linear dependence on inelasticity convoluted with a gaussian distribution describing the known experimental resolution and these fits were extrapolated to the elastic region (e.g. full line in Fig. 2). The amount of background within the elastic region defined by cut (1) was estimated independently for each target and Q^2 bin. Within statistical errors we observe no target material or Q^2 dependence. The amount of background averaged over all data is 0.23 ± 0.11. The EMC NA9 experiment, which covered a wider momentum range with almost 4π acceptance for hadrons, observed a similar level of background. It was found [2] that the sample of events satisfying selections similar to ours and classified as exclusive ρ^0 events contained at least 14% of events with low momentum hadrons not detected by the forward spectrometer.

The main contribution to the error comes from the uncertainty of the extrap-

[1]Due to smearing, for a fraction of events the measured M_X is smaller than the nucleon mass M_p. To avoid problems with unphysical kinematics, for these events it was assumed that $M_X = M_p$.

olation into the low I region. This uncertainty was estimated to be about 50%. The uncertainty of background estimates from fragmentation models is of the same order [7].

Using the estimated amount of background and the background slope, the slopes b_{ex} were fitted to the data in different Q^2 bins. However, with this inelasticity cut the non-negligible level of background with its large uncertainty results in unacceptably large errors on the fitted b_{ex} values.

To reduce the background in the sample in order to make a useful determination of b_{ex} we introduced a more restrictive cut

$$-0.05 < I < 0.00. \tag{4}$$

To improve statistics the data at both energies and for the Q^2 range 6 – 25 GeV^2 were combined. In this kinematic range no incident muon energy or Q^2-dependence is seen (Fig.5).

After introducing the large Q^2 cut and the inelasticity cut (4) the sample consists of 218 events taken at muon energy 200 GeV and 81 events at 280 GeV. The measured slope is $b = 4.0 \pm 0.5$ GeV^{-2}. This value is measured at $< Q^2 >=$ 9.3 GeV^2 and $< \nu >=$ 105 GeV. It was estimated that the amount of background in the region $I < 0$ was 0.04±0.04 due to smearing from the region $I > 0$. The extracted slope for exclusive events is then $b_{ex} = 4.3 \pm 0.6$ GeV^{-2}, where the error is statistical. To estimate the systematic error due to the background, b_{bk} was varied within the limits 1.1 – 2.5 GeV^{-2}. These limits correspond ($b^{-1} =< p_t^2 >$) to a range of 0.4 – 0.9 GeV^2 in $< p_t^2 >$, a larger range than the one observed for inclusive hadrons in a comparable kinematical region [15]. The systematic error on b_{ex} due to the background is (+0.47,–0.20) GeV^{-2}. The more restrictive cut on the inelasticity (4) was essential to keep this error small. In addition other experimental uncertainties (momentum calibration, acceptance corrections) contribute 0.6 GeV^{-2} to the systematic error. Then the p_t^2- slope for exclusive ρ^0 production at high Q^2 is $b_{ex} = 4.3 \pm 0.6 \pm 0.7$ GeV^{-2}, where the first error is statistical and the second the total systematic one.

This result is substantially higher than the values 1 – 2 GeV^{-2} measured by the EMC at large Q^2. We think that two factors related to the analysis contribute to this discrepancy. First, using p_t^2 instead of t' allows us to avoid kinematic uncertainties related to the semi-exclusive character of the data. Second, with higher statistics in the present experiment it was possible to make more restrictive cuts on the inelasticity and therefore to reduce the amount of background.

The present data indicate that the mechanism of exclusive ρ^0 muoproduction is different to that of inclusive hadrons produced in hard scattering processes. The obtained slope of 4.3 GeV^{-2} corresponds to a mean p_t^2 of $0.24 \pm 0.04 \pm 0.04$ GeV^2. This value is substantially higher than the mean p_t^2 of 0.6 – 0.7 GeV^2 for leading (high z value[2]) inclusive hadrons produced in deep inelastic scattering in a comparable

[2] z is the fraction of the virtual photon energy taken by a hadron. For the exclusive ρ^0s the following approximate relation holds: $z \simeq 1 - I$.

Q^2 and W^2 range [15]. On the other hand, the present data are compatible with predictions of a model [4] which assumes that the pomeron exchange is dominant in exclusive ρ^0 production. For similar kinematic ranges this model predicts slopes in the range 5 – 6 GeV^{-2} [16].

Summary and Conclusions

We have measured p_t^2- and t'-slopes for exclusive ρ^0 muoproduction on different targets at large Q^2. The Q^2 range was extended with respect to previous experiments and our exclusive ρ^0 sample is about four times as large. The slopes for production on hydrogen and incoherent production on nuclei are all equal within statistical errors.

When similar cuts and selections are used in the data analysis, our results on the t'-slopes agree with those from the previous experiments. For the non-exclusive background events the variable t' is, however, wrongly determined if the nucleon mass is used for that of the recoiling system; this distorts the t' distributions. The variable p_t^2 is free from the uncertainty of the recoiling mass and we have shown that the Q^2 dependence of the p_t^2-slope is weaker than that of the t'-slope. At large Q^2 the p_t^2-slope is constant. To reduce the non-exclusive background, in order to make a precise determination of the p_t^2-slope b_{ex} for exclusive ρ^0 production, we imposed a restrictive inelasticity cut. For the combined large Q^2 data we then obtain a slope $b_{ex} = 4.3 \pm 0.6 \pm 0.7$ GeV^{-2} at $< Q^2 >= 9.3$ GeV^2.

The p_t^2 distributions of exclusive ρ^0 muoproduction at large Q^2 measured in this experiment are much softer than those for the production of leading inclusive hadrons in deep inelastic scattering. This is in contradiction to the earlier conclusion [2]. The present result is compatible with the model of ref. [4] which assumed the dominance of pomeron exchange for this process and has been used to deduce the pomeron "size".

We wish to thank the technical staff of CERN and of the participating institutions for their invaluable contributions to the experiment. We are also grateful to J.R.Cudell, A.Donnachie and P.V.Landshoff for comments and suggestions.

References

1. T.H.Bauer *et al.*, Rev.Mod.Phys.**50**,No.2(1978)261.
2. EMC,J.J.Aubert *et al.*, Phys.Lett.**B161**(1985)203.
3. EMC,J.Ashman *et al.*, Z.Phys.**C39**(1988)169.
4. A.Donnachie and P.V.Landshoff, Phys.Lett.**B185**(1987)403.
5. S.J.Brodsky, SLAC-PUB-5013(1989).
6. A.Donnachie and P.V.Landshoff, Nucl.Phys.**B311**(1989)509.
7. J.R.Cudell, Nucl.Phys.**B336**(1990)1.
8. P.V.Landshoff, Nucl.Phys.B(Proc.Suppl.)**18C**(1990)211.
9. NMC,D.Allasia *et al.*, Phys.Lett.**B249**(1990)366
   and references cited therein;
   NMC,P.Amaudruz *et al.*, CERN-PPE/91-167(1991),
   to be published in Nucl.Phys.
10. NMC,P.Amaudruz *et al.*, Z.Phys.**C51**(1991)387.
11. Particle Data Group, Phys.Lett.**B239**(1990)III.48.
12. EMC,O.C.Allkofer *et al.*, Nucl.Instr.Meth.**179**(1981) 445.
13. J.D.Jackson, Nuovo Cimento **34**(1964)1644.
14. Particle Data Group, Phys.Lett.**B239**(1990)II.4.
15. EMC,J.Ashman *et al.*, CERN-PPE/91-53(1991);
    EMC,J.J.Aubert *et al.*, Phys.Lett.**B95**(1980)306.
16. J.R.Cudell, A.Donnachie and P.Landshoff, private communication.

Figure Captions

Fig. 1 Acceptance corrected distribution of the two-pion invariant mass.The data are for muon scattering on deuterium at 200 GeV and satisfy the cuts listed in Table 1 and the inelasticity cut (1). The full line is a result of a fit assuming a superposition of a ρ^0 p-wave Breit-Wigner and a non-resonant contribution. The broken line shows the non resonant contribution parametrised as $B(m_{\pi\pi}) = a_0(m_{\pi\pi} - 2M_\pi)^{a_1} e^{-a_2 m_{\pi\pi}}$, where a_0, a_1, a_2 are fitted parameters and M_π is the pion mass.

Fig. 2 Inelasticity distribution uncorrected for acceptance. The data are for muon scattering on deuterium at 200 GeV and satisfy the cuts listed in Table 1 and the invariant mass cut (2). The solid line represents the parameterisation of the non-exclusive background described in the text.

Fig. 3 The p_t^2 distributions for selected targets and Q^2 ranges.

Fig. 4 The p_t^2-slopes for different targets as a function of Q^2.

Fig. 5 Comparison of the p_t^2-slopes (full symbols) and t'-slopes (open symbols). t' was calculated assuming the nucleon mass for the recoil system. The data from different targets are combined.

Fig. 6 Comparison of the t'-slopes measured in this experiment with those from refs. [2,3].

Fig. 7 Effect of two assumptions on the mass of the recoiling system on the t'-slopes. The open symbols correspond to t_{min} calculated assuming the nucleon mass, the full symbols to t_{min} calculated assuming the measured missing mass.

Fig. 8 The measured p_t^2-slope as a function of inelasticity. The data for $6 < Q^2 < 25$ GeV^2 and for both incident muon energies are combined.

Table 1

Kinematic cuts applied to the data sample
($E_{\mu'}$ is the energy of scattered muon, p_h the hadron momentum)

Icident muon energy [GeV]	200	280
Q^2_{min} [GeV^2]	2	3
ν-range [GeV]	40 – 190	60 – 260
y_{max}	0.9	0.9
$E^{min}_{\mu'}$ [GeV]	20	20
p^{min}_h [GeV]	4	5

Table 2

Numbers of exclusive ρ^0 events in the data samples
after applying the cuts listed in Table 1 and cuts (1) and (2)
defined in the text

Incident muon energy	Target material				
	H	D	C	Ca	All
200 GeV	–	583	269	433	1285
280 GeV	96	234	–	–	330
					1615

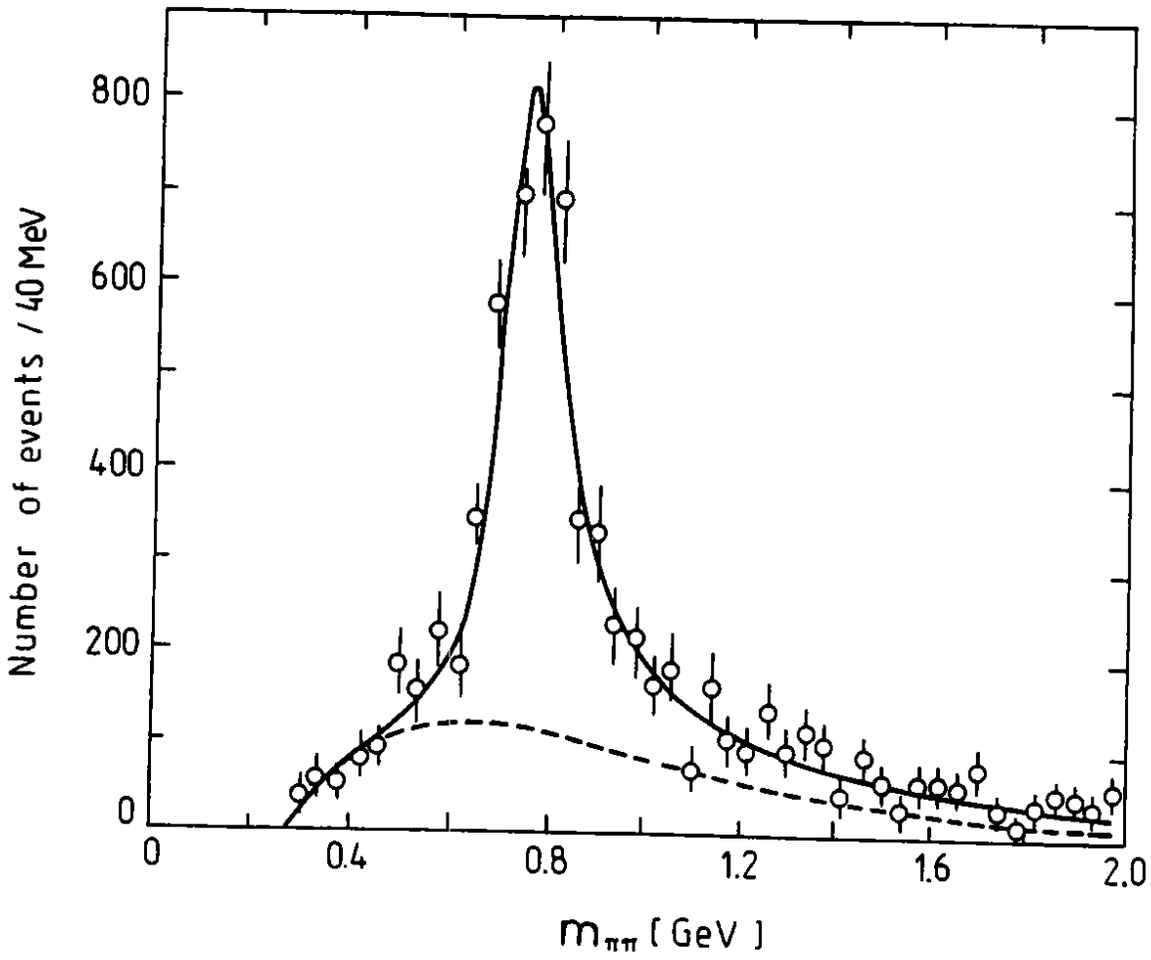
800
600
400
200
0
Number of events / 40 MeV
0
0.4
0.8
1.2
1.6
2.0
$m_{\pi\pi}$ [GeV]

Fig. 1

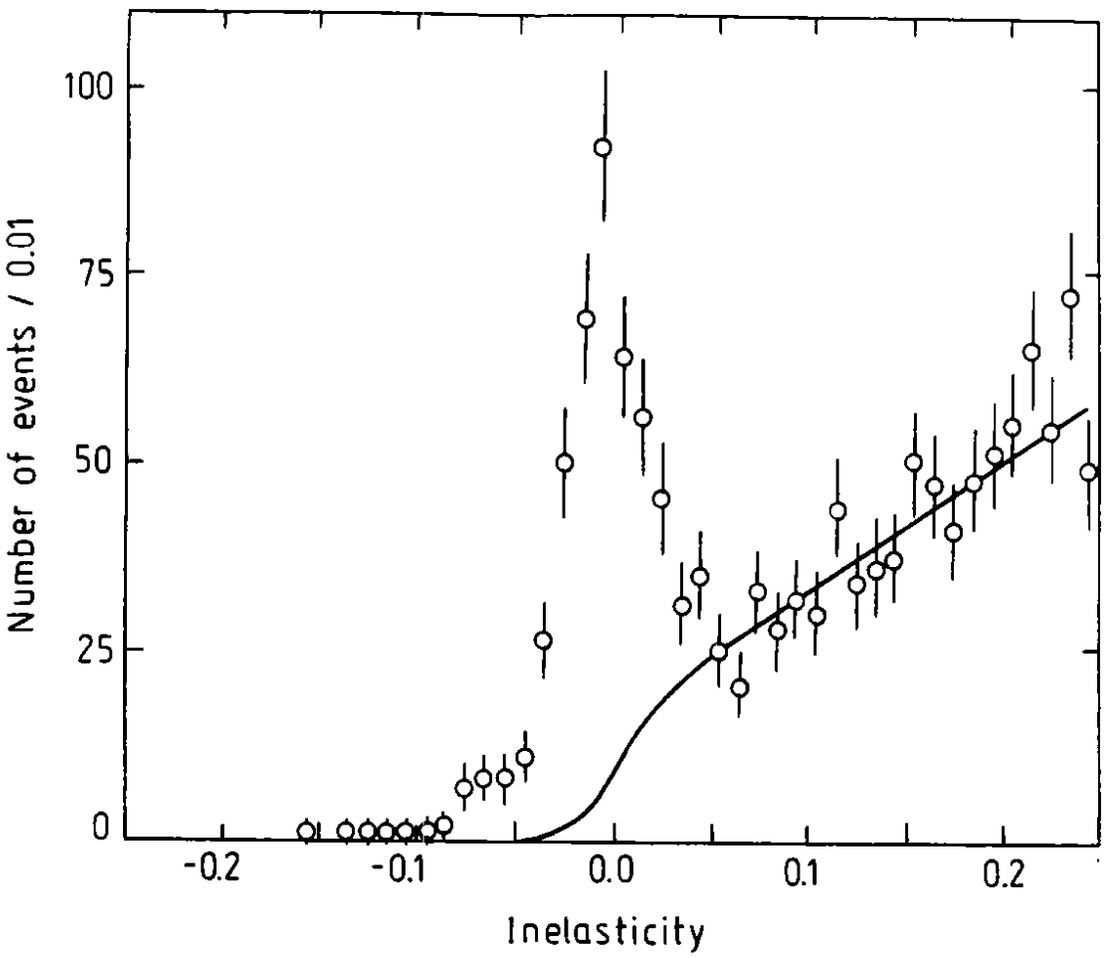

Fig. 2

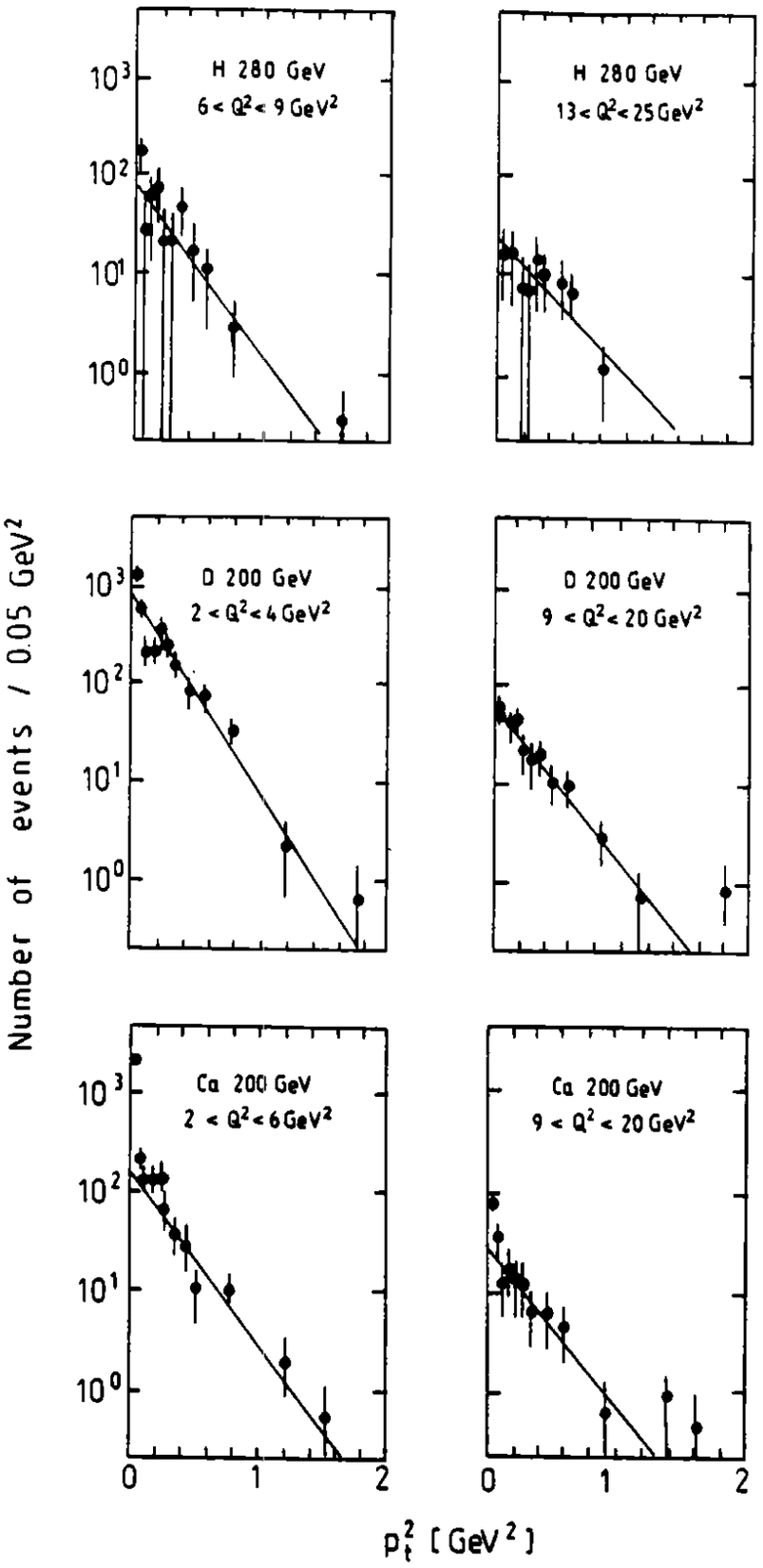
H 280 GeV
6 < Q² < 9 GeV²
H 280 GeV
13 < Q² < 25 GeV²
D 200 GeV
2 < Q² < 4 GeV²
D 200 GeV
9 < Q² < 20 GeV²
Ca 200 GeV
2 < Q² < 6 GeV²
Ca 200 GeV
9 < Q² < 20 GeV²
Number of events / 0.05 GeV²
p_t² [GeV²]

Fig. 3

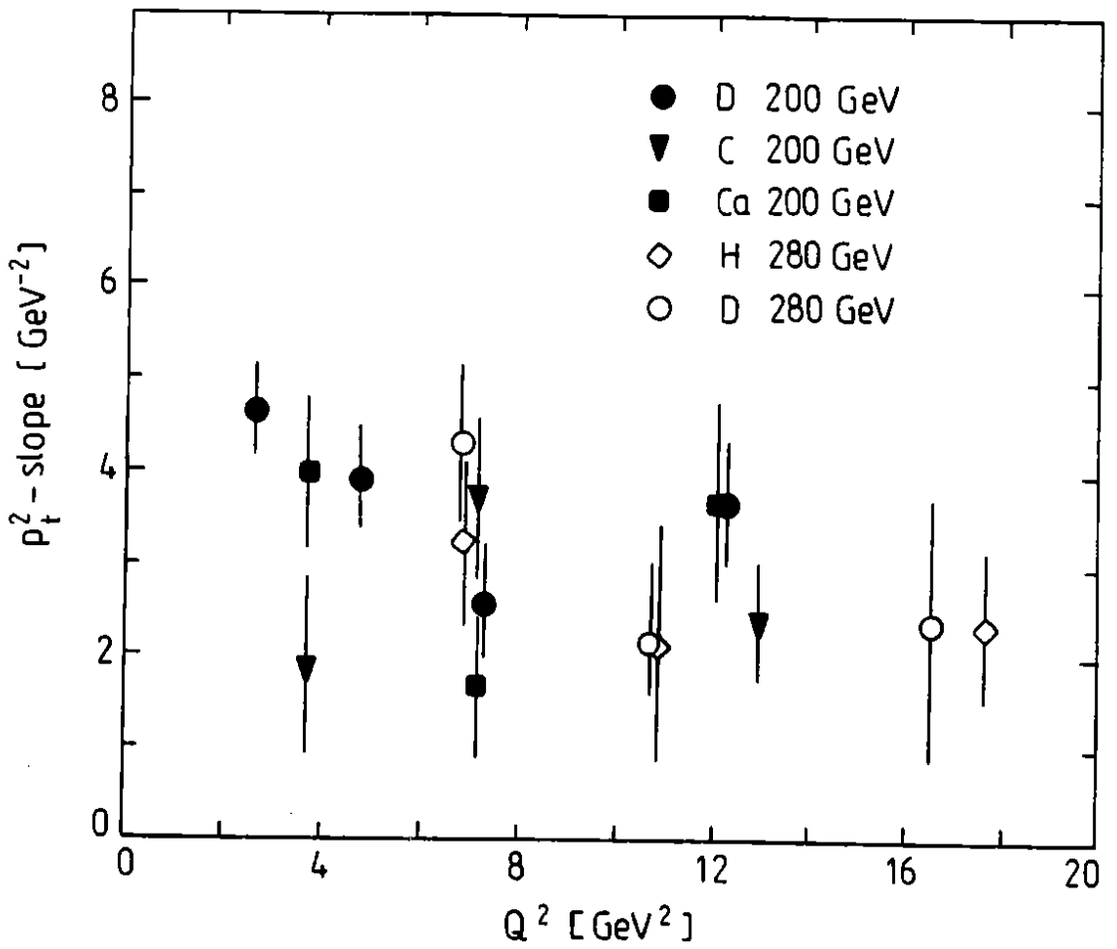
D 200 GeV
C 200 GeV
Ca 200 GeV
H 280 GeV
D 280 GeV
p_t^2 - slope [GeV^{-2}]
Q^2 [GeV^2]
0
2
4
6
8
0
4
8
12
16
20

Fig. 4

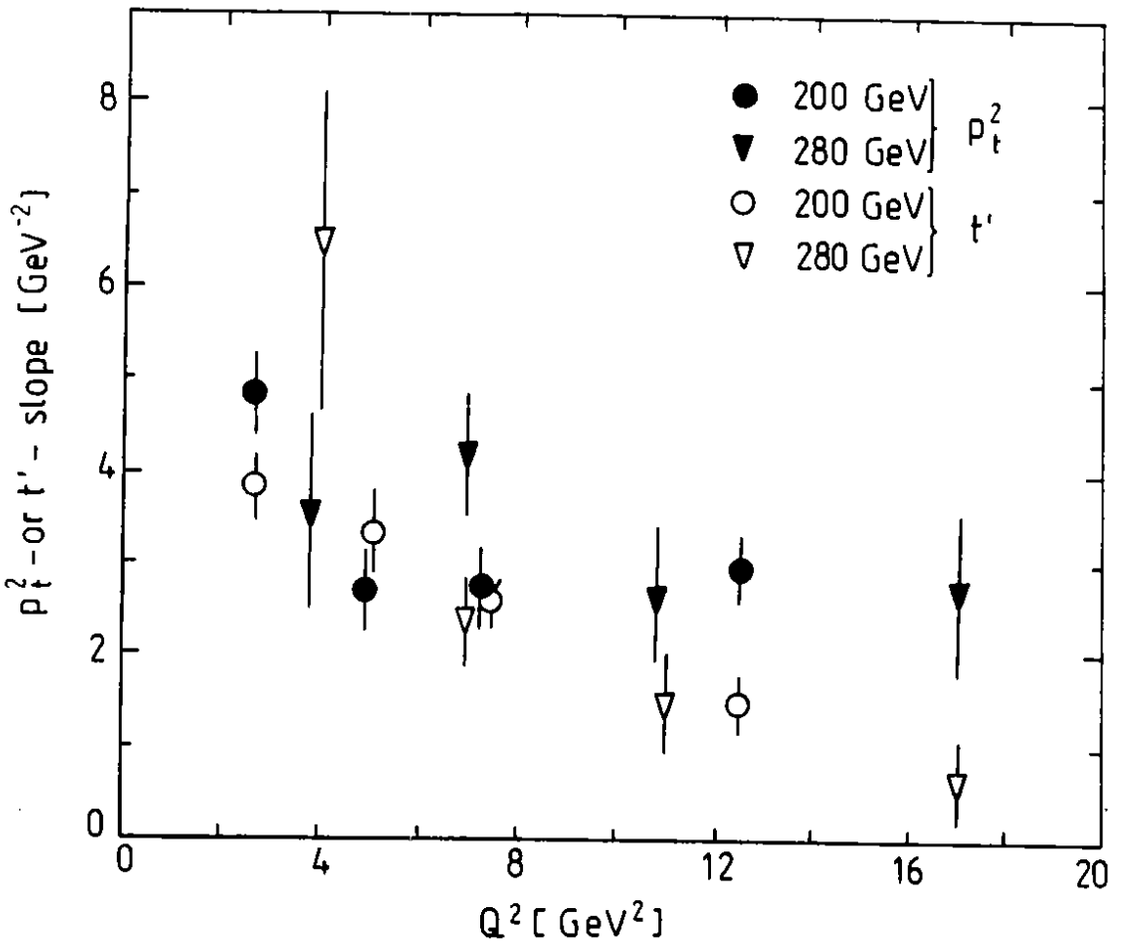
200 GeV
280 GeV
p_t^2
200 GeV
280 GeV
t'
p_t^2 -or t' - slope [GeV^{-2}]
Q^2 [GeV^2]
0
2
4
6
8
0
4
8
12
16
20

Fig. 5

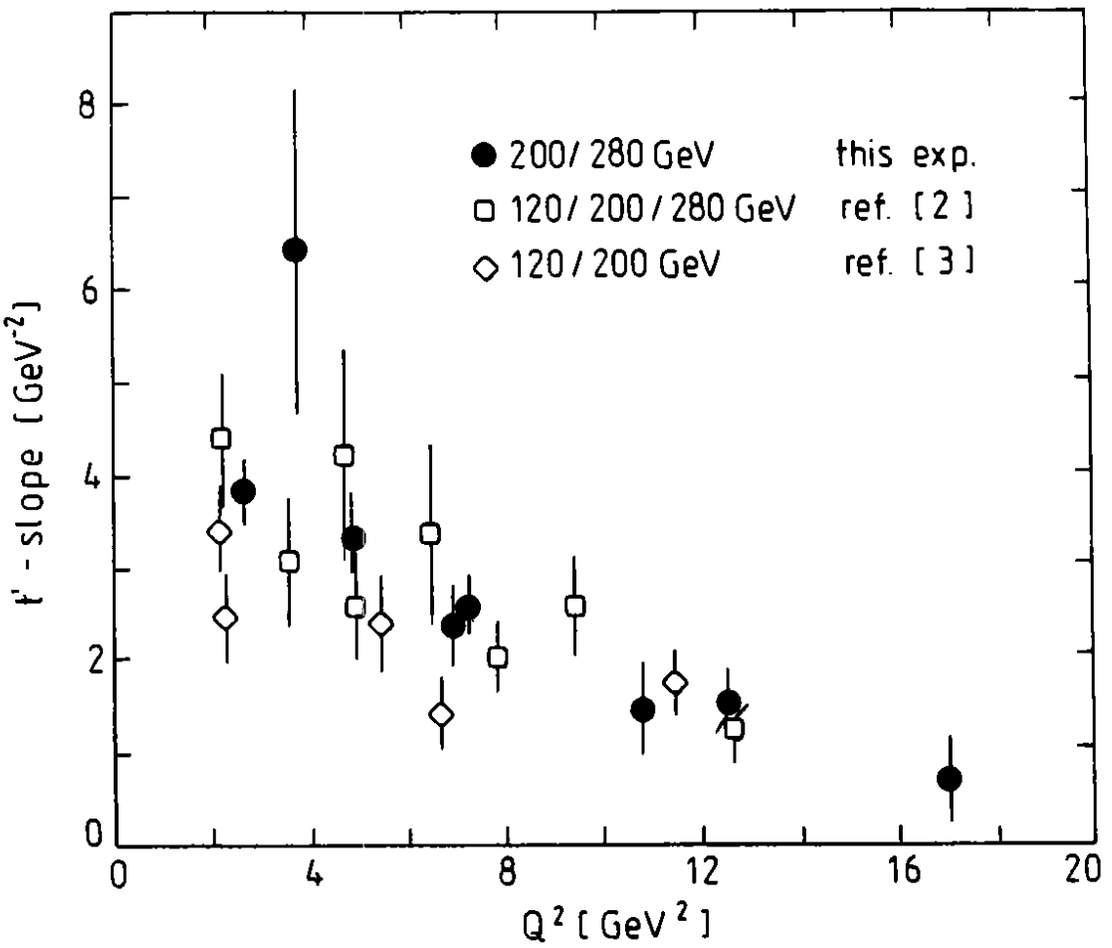
● 200/ 280 GeV this exp.
□ 120/ 200 / 280 GeV ref. [2]
◇ 120 / 200 GeV ref. [3]
t' - slope [GeV⁻²]
Q² [GeV²]
0
2
4
6
8
0
4
8
12
16
20

Fig. 6

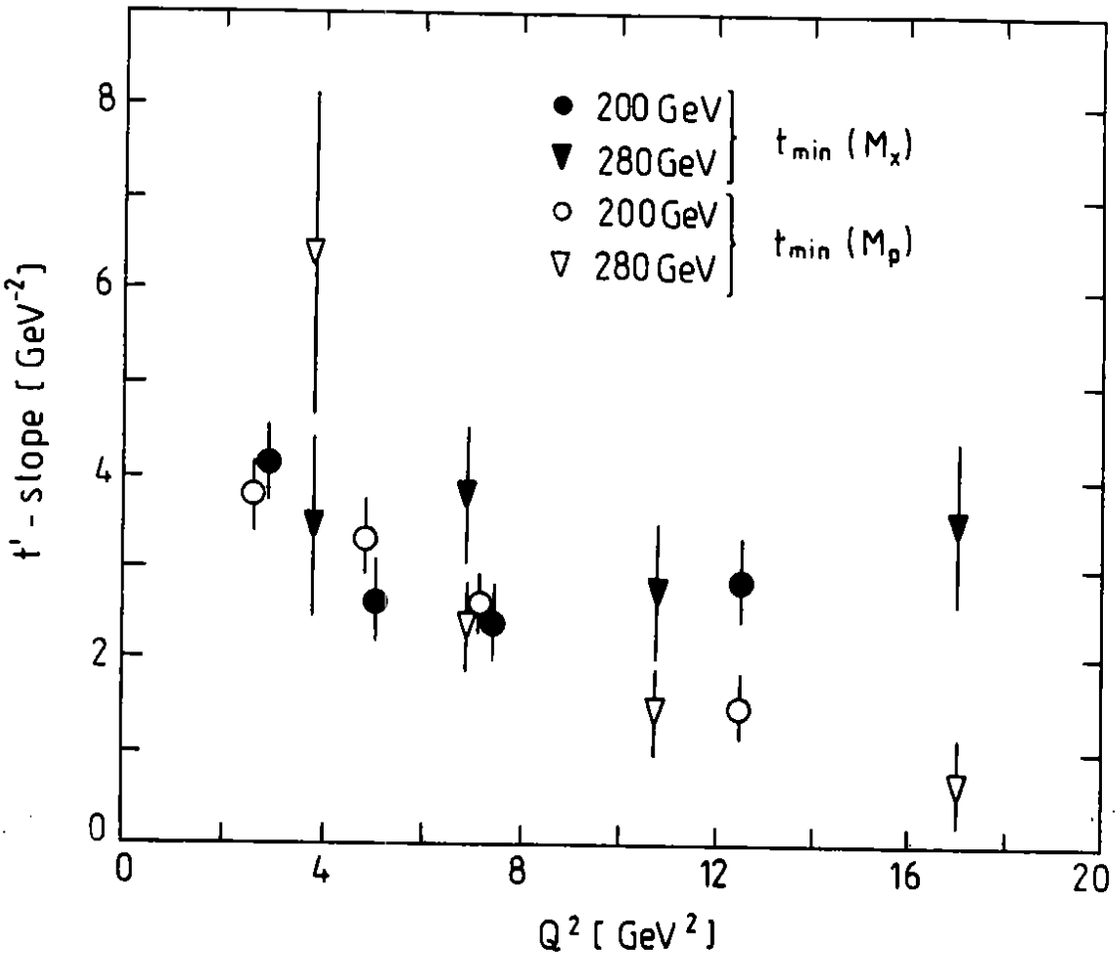
200 GeV
280 GeV
t_{min} (M_x)
200 GeV
280 GeV
t_{min} (M_p)
t' - slope [GeV^{-2}]
Q^2 [GeV^2]
0
2
4
6
8
0
4
8
12
16
20

Fig. 7

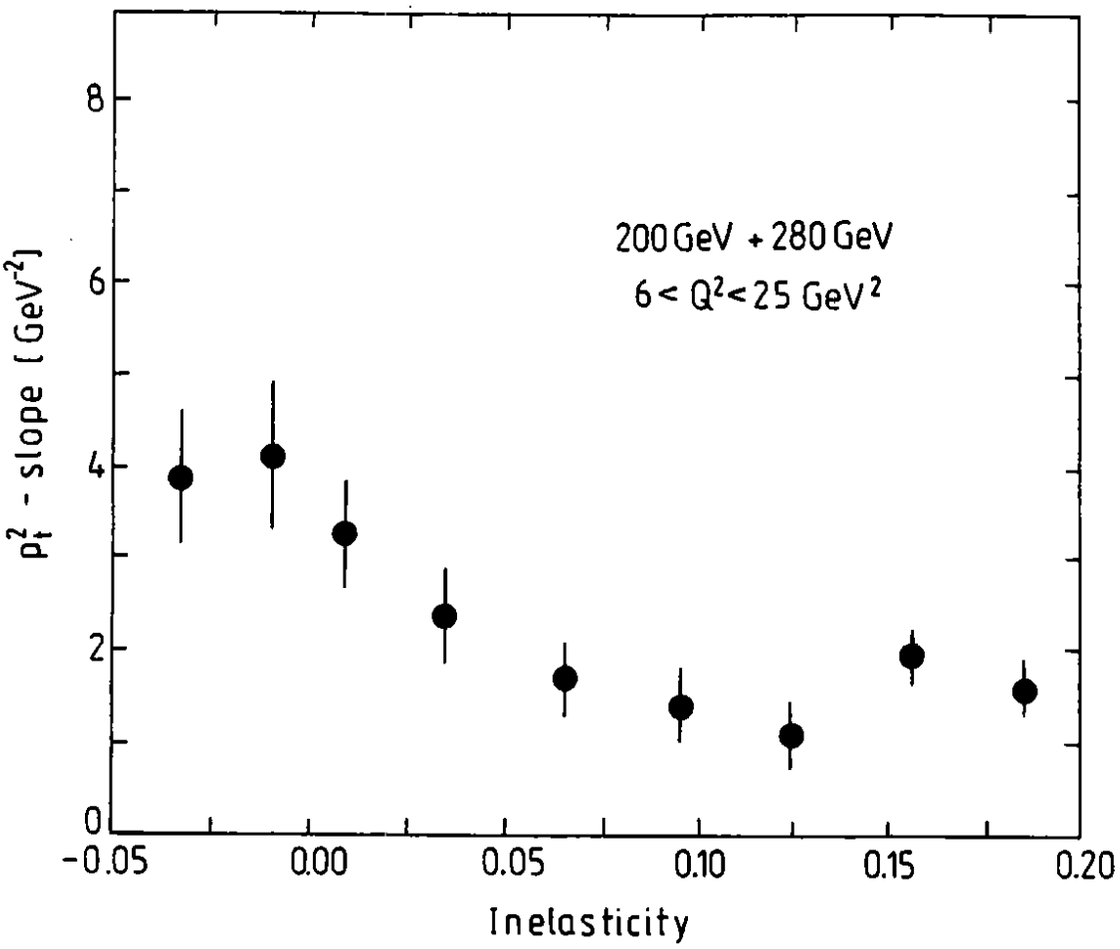

Fig. 8

Imprimé au CERN. Prix : 0.60 Fr.